RARE METALS

MINI REVIEW

Metal-containing covalent organic framework: a new type of photo/electrocatalyst

Xiao-Tong Wang, Xiao-Feng Lin* , Ding-Shan Yu*

Abstract Metal-containing covalent organic frameworks (MCOFs), as a class of crystalline organic polymers with abundant single-atom metal sites, can respond effectively to various vital reactions, including hydrogen evolution reaction (HER), CO_2 reduction reaction (CO_2RR), oxygen reduction reaction (ORR) and oxygen evolution reaction (OER). The advent of MCOFs provides a platform for the establishment of model catalysts with highly repetitive structure to facilitate theoretical calculations and high-throughput screening while designing flexibility in monomer construction to lay the foundation for the development of highly selective and active photo/electrocatalysts. In this review, we summarize the recent progress in this field and highlight several important MCOFs photo/electrocatalysts for OER, ORR, HER, and CO_2RR. Moreover, various approaches are also mentioned to improve or optimize the catalysts and indicate the future research direction on enhancing the performance of MCOFs catalysts based on the current existing challenges.

1 Introduction

In recent decades, the pursuit of renewable energy stimulates the development of advanced catalytic material in photo/electrochemical reactions, like the hydrogen evolution reaction (HER), oxygen reduction/evolution reaction (ORR/OER), and CO_2 reduction reaction (CO_2RR). However, these photo/electrochemical reactions are important chemical transformation processes that carry on renewable energy conversions, in which the activity, selectivity, and stability of electrocatalysts play a vital role in determining the energy efficiencies and overall system performance [1–10]. Almost in parallel (or slightly later) to its rise in metal-organic framework (MOFs) catalysis, the concept of covalent organic framework (COFs) has been introduced into the field of photo/electrocatalysis [11, 12]. Different from MOF, the monomers of COF are usually connected by covalent bonds to get better stability in its framework. Among them, metal-containing COF (MCOFs) is more favored by researchers and it can be divided into two main categories, that is, immobilized molecular catalysts and re-coordinated metal base catalysts [13–20]. Containing metal elements are mainly transition metals such as ruthenium (Ru), iron (Fe), cobalt (Co), copper (Cu), and nickel (Ni). They are dispersed as single atoms on organic framework-based conductive substrates and usually stabilized via bonding with nitrogen dopants or other heteroatomic species [21, 22]. It is the covalently coordinated transition metal centers that find promising adsorption properties and

X.-T. Wang, D.-S. Yu*
Key Laboratory for Polymeric Composite and Functional Materials, Ministry of Education, Sun Yat-Sen University, Guangzhou 510275, China
e-mail: yudings@mail.sysu.edu.cn

X.-T. Wang, D.-S. Yu
Key Laboratory of High Performance Polymer-based Composites, Guangdong Province, School of Chemistry, Sun Yat-Sen University, Guangzhou 510275, China

X.-F. Lin*
School of Chemical Engineering and Light Industry, Guangdong University of Technology, Guangzhou 510006, China
e-mail: linxf9@gdut.edu.cn

stability, with the latter probably even more critical in acid electrolytes, of such non-precious elements for photo/electrocatalytic applications [23–28].

In general, electrocatalytic reactions are taking place at the solid–liquid interface or the solid/liquid/gas interface. The double-layer (DL) structure of the electrode/solution interface, the free energy of the reactants/products, and the corresponding adsorption energy change significantly with the variation of the potential of the working electrode [29–32]. The pivotal role of electrocatalyst is to provide the main reaction site as well as the microenvironment, and its catalytic performance is inextricably linked to surface science [33–35]. The pursuit of ideal electrocatalysts with high activity, selectivity, and durability has been driving the interdisciplinary integration of heterogeneous catalysis and coordination chemistry. In the last couple of decades, several important developments have taken place as a result of using the conceptual framework of coordination chemistry to understand the catalytic mechanism and to improve the design of heterogeneous metal catalysts [36, 37]. First of all, the development of single-atom catalysts (Fe–N–C, Co–N–C, Mn–N–C, etc.) makes researchers recognize the vastly different properties of single-atom catalysts versus bulk materials and they try to establish structure–function relationship from a coordination chemistry perspective [21, 38–40]. The second point is the emergence of modern surface science and the combination of high-energy spectroscopic techniques (e.g., Mossbauer spectrum, X-ray absorption spectroscopy, etc.). Consequently, Co-containing MCOFs as model catalysts has made it possible to probe the atomic structure of catalytic surfaces and to characterize how reactants are activated and converted to products on these surfaces, allowing us to gain insight into complex heterogeneous catalysis [41–44]. The ligand bond structure of reactants and intermediates has been widely shown to be related to the surface structure of model catalysts and is critical to catalytic performance. Thus, the term that "surface coordination chemistry" naturally entered practice along with the concept of "ligand-unsaturated sites" [45, 46]. Although initial instructive explorations proposed valuable ideas for single-atom catalyst design, the means of regulation as well as the establishment of conformational relationships remained great challenges. However, the advent of MCOF provided an opportunity for the establishment of model catalysts with highly repetitive structural units to facilitate theoretical calculations and high-throughput screening, and high design flexibility in monomer construction to lay the foundation for the development of electrocatalysts with selectivity and activity [47–50].

Photocatalysis is direct use of light for energy conversion, which is a chemical reaction of substances under the co-action of light and catalyst. When the photon energy is greater than or equal to the energy bandgap of the photocatalyst under light conditions, the photocatalyst is excited to produce photogenerated electrons and holes, where the electrons are excited to the lowest unoccupied molecular orbital (LUMO) and the holes are stay on the highest occupied molecular orbital (HOMO) [51, 52]. Then, the separation of electrons and holes occurs, after which the electrons or holes continue to migrate to the surface of the photocatalyst for reduction and oxidation reactions, respectively. From the basic principles of photocatalysis, broadening the spectral response range and improving the photogenerated electron–hole lifetime are two main ways to improve the visible photocatalytic performance of semiconductors [53, 54]. Regulating the energy band structure of semiconductors is a common method to broaden the spectral response range, and from the perspective of energy band structure, modulation methods can be divided into valence band modulation, conduction band modulation, and simultaneous valence/conduction band modulation [55–57]. MCOFs with large π-conjugated system can serve as a photosensitizer to enhance the absorption of light and increase the number of electron–hole pairs generated under solar illumination, which leads to the expansion of effective light capture and light contact area [27, 28, 58, 59]. Especially, the formation of a large π-conjugated system with the D-A organic linker significantly enhances the photoreactive performance of MCOFs [60–63]. The porous structure allows MCOFs to have more exposed active metal sites and transport channels for catalytic substrates and products, which is conducive to the rapid transfer and utilization of photogenerated charges [64]. The metal sites of MCOF are strongly adsorbed and can be considered as the predominant reaction sites, and their catalytic properties are influenced by the spin state of the metal, the oxidation state, and other factors [14, 25].

Organometallic chemistry developed under the conceptual framework of classical coordination chemistry already provides core foundations for the field of MCOFs catalysis [65, 66]. The structure of MCOFs in photo/electrocatalysis has been generalized, ranging from coordinated metal atoms to anchoring organic framework and traditional porphyrin-based COF, with various 3d–5d transition metals being investigated as the active centers (Fig. 1). In addition to the enhanced reaction (high turnover rates) and mass (high metal utilization efficiency) activities, attention has been devoted to tailoring the catalytic selectivity by taking advantage of the atomic-scale modulation of adsorption for reaction intermediates [67–71]. This review aims to summarize the progress made over the past years on the development of MCOFs-based photo/electrocatalysts. In recognition of the unique structure and property, their distinct catalytic performance will be the top priority of this article.
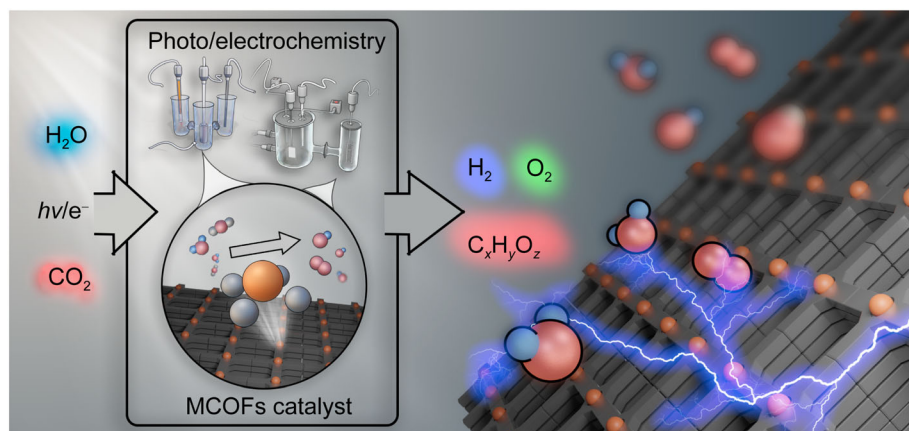
Fig.1 Schematic illustration of conversion technology based on MCOF-based photo/electrocatalysts for OER, ORR, HER and CO_2RR

2 Synthesis of MCOFs

MCOF is a small branch of COF, which allows metal ions to anchor to a specific structure through coordination bond is based on the framework of COF. Thus, it can be seen that the in-depth understanding of the MCOF should be based on insight into the structure of the COF [64, 72]. As we know, the common synthesis of COF is a bottom-up approach to construct a repeating network structure by connecting "knots" and "links", so it is the same in the process of most porphyrin/phthalocyanine MCOFs [73–75]. However, some specific MCOFs can be constructed in the top-down method, that is, the target structure bonds the N on the backbone to the metal atom through coordination bonds [76].

2.1 Basic structure of COFs

COF is a class of crystalline porous polymers which allow atomically precise integration of organic to build units for creating order skeletons in a repetitive manner [67]. According to the topology, COFs materials can be divided into two categories, that is, two-dimensional COFs and three-dimensional COFs (Fig. 2). In the two-dimensional COFs, the monomers are connected by covalent bonds to form a laminar structure in the plane, with the layers forming a conjugated system through π-π interactions, so the size and shape are closely related to how its layers are stacked. However, different from the two-dimensional COFs, the three-dimensional COFs tend to form larger cage-like cavities, and the monomer can continue to react and grow outwards, then shape a multiple interspersed structure [77]. The base unit of COFs can be described in terms of "knots" and "links", but their connections are limited by the innate structure of the monomer and the reaction conditions. The common connection structures are some linkages, such as boroxine boronate-ester,
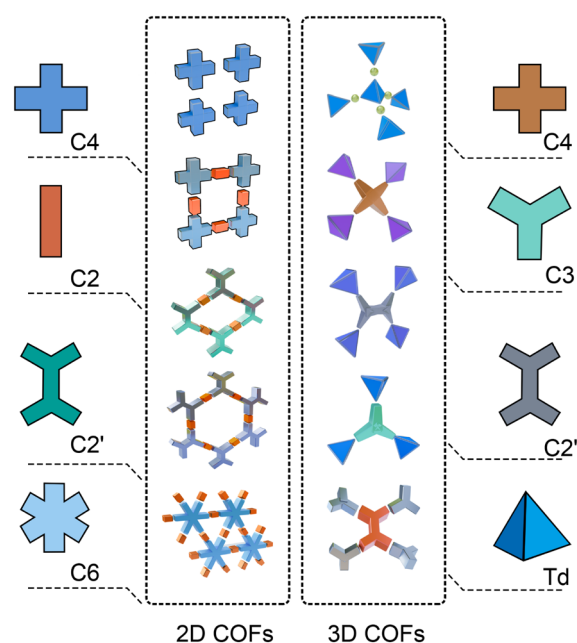

Fig. 2 Different types of symmetric combinations used for 2D and 3D COF construction

borosilicate, triazine, imine, hydrazone, borazine, squaraine, azine, phenazine, imide, spiroborate, C=C, amide, and viologen [14]. The skeletal structure of COFs is determined by the structural units and the type of connection. To date, studies of COFs have collected a wide range of different topologies of 2D and 3D structures, which use the building block with different shapes, geometries, and functions [26].

2D COFs can be built with their different blocks or combinations. Several structural topologies have been accessed in 2D COFs, that is, hcb (honeycomb), sql (square lattice), kgm (kagome), hxl (hexagonal), fxt, kgd (kagome-dual). The structural units of metal-base porphyrin COFs are usually combined in the form of (C4 + C2) [28]. For

instance, Yusran and co-workers [77] prepared 2D COF which was synthesized by employing a linear building block of hydroxyl-containing 4,4′-(1,2-ethynediyl) bis-2-hydroxybenzaldehyde and the square-shape 5,10,15,20 - tetrakis (4-aminophenyl) porphyrin as the basic backbone, and it possesses AA layer-stacking mode with 3.3-nm predicted 1D square-like open channel.

Compared with 2D COFs, most 3D COFs are composed of tetrahedral-shaped components tetrahedral-like building blocks (Td). Based on the topological map, 3D COFs can be divided into different networks, including cnt, dia, srs, rra, ffc, ctn and bor networks, which can be realized by the [Td + C3] diagram and provide the skeleton without the penetration to get large surface areas [27, 28, 58]. Also, the network can be generated by a [Td + Td] diagram. The dia network is designed by the [Td + C2] diagram. It constitutes the largest 3D COF series because of its wide representation diversity of connected units. And the combination of tetrahedral (Td) knots such as tetrakis-(4-aminophenyl) methane (TAPM) and linear C2 linkers (e.g., terephthalaldehyde, succinic anhydride) (Td + C2 and Td + Td combinations) create 3D COFs with diamondoid (dia) topology [78].

2.2 Preparation strategies of MCOFs

The common MCOFs mainly exist in 2D COF form and its synthesis is divided into two ways: bottom-up and top-down approaches [72]. The former one is to realize the introduction of metal atoms through the design of basic monomers. To give an obvious example, the porphyrin COF with Fe, Zn, Co, etc. whose porphyrin units at the nodes of mesoporous framework often plays the role of "knots" and combines with other "links" to form a topological network, and it is prepared by common wet chemical methods such as the solvothermal synthesis, microwave-assisted synthesis, aqueous synthesis, and interfacial synthesis [14]. These methods are basically similar to traditional COF synthesis but only differ in the choice of monomers. However, the latter one is to synthesize the designed COF structure first, and then realize the target construction through the later adsorption of metal ions/metal-containing small molecules to obtain MCOFs. This process commonly uses inorganic salts and metal–organic complexes as a metal source, anchored directly to the skeleton by moderate conditions. For example, Zhong et al. [79] prepared Ni-DBA-2D-COF for the reductive cleavage of inert aryl C-S bonds, and 2, 2′-bipyridine-based COF (TpBpy) was treated with Ni $(ClO_4)_2 \cdot 6H_2O$ in acetonitrile. The solid was filtered and washed with copious amount of acetonitrile and dried in vacuum at 60 °C overnight to give Ni-TpBpy. Single Ni sites were successfully anchored in TpBpy through the chelation of

bypridine binding units. They proposed a new azine-linked 2D COF containing nickel-doped dehydrobenzoannulene (DBA) units by combining DBA, Ni $(COD)_2$, and toluene and stirring them overnight. The resulting suspension quickly changed from yellow to dark blue during this time. Hexanes were added to the solution and the solids were collected by vacuum filtration, then washed with hexanes to yield Ni-DBA as dark blue solids [80]. DBAs are planar triangular-shaped macrocycles, so they can use their soft alkynyl ligands to form complexes with low oxidation state transition metals. The top-down approach offers a good deal of flexibility, but the type of metal ion and thermodynamic stability must be considered.

3 Applications in photocatalyst

3.1 MCOFs-based photocatalyst for CO_2RR

CO_2 is one of the most stable molecules because of the strong C=O double bond with a bond energy of 750 kJ·mol^{-1}, significantly larger than those of C–C (336 kJ·mol^{-1}), C–O (327 kJ·mol^{-1}) or C–H bonds (411 kJ·mol^{-1}) [81, 82]. The CO_2RR by electrocatalytic or photocatalytic method is a thermodynamically uphill reaction that requires a large energy input to break the C–O bond. To complicate matters further, CO_2 reduction may proceed through several different reaction pathways, transfer 2, 4, 6, 8, 12, or even more electrons and produce different reduction products, including carbon monoxide (CO), formic acid (HCOOH), methane (CH_4), ethylene (C_2H_4), etc., depending on the nature of the electrocatalyst or photocatalyst and the actual experimental conditions [83, 84]. Therefore, electrocatalytic or photocatalytic CO_2 reduction generally suffers from limited efficiency and poor selectivity.

Figure 3a shows a typical process of photocatalytic CO_2 reduction on a semiconductor photocatalyst, which involves five sequential steps—light absorption, charge separation, CO_2 adsorption, surface redox reaction, and product desorption [85–87]. The first step is the absorption of photons to generate electron and hole pairs. The electrons are excited from the valence band (VB) to the conduction band (CB) under illuminating and the same number of holes are left in VB [88]. For these photogenerated electrons or holes to be energetically favorable to reduce CO_2, photocatalysts should possess suitable band structure, so CB edge must be more negative than the redox potential of CO_2RR, and the VB edge should be more positive than the redox potential of CO_2RR (−0.52 V (vs. SHE) in pH 7.0) [89, 90]. The bandgap must be sufficiently suitable since we need to additionally take into consideration of the large overpotentials associated with these two
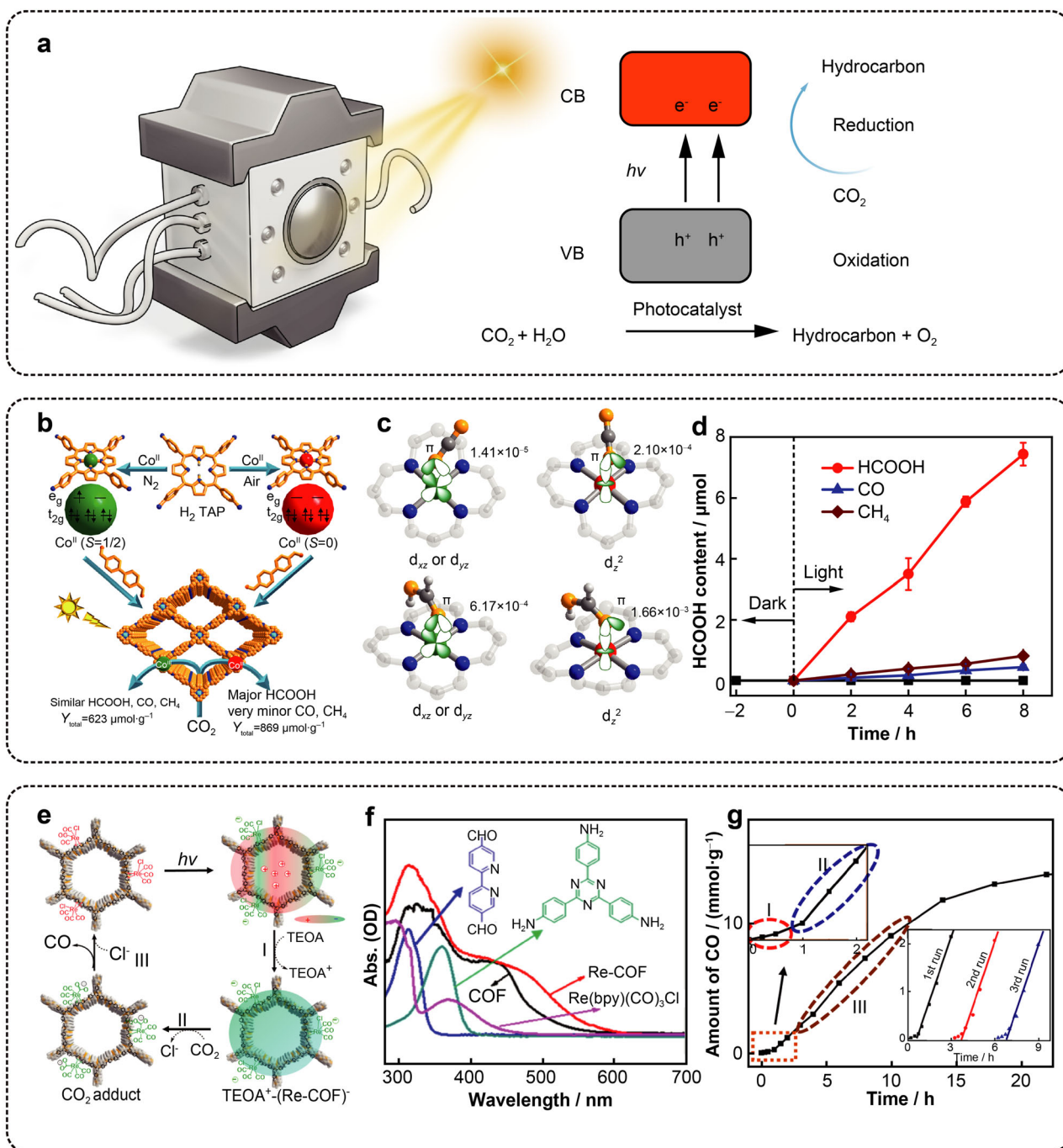
Fig. 3 a Schematic diagram of photocatalytic test system and photocatalytic mechanism; **b** rational fabrication of COF-367-Co featuring different spin states of Co ions toward photocatalytic CO_2RR; **c** different coupling modes of CO_2 and HCOOH interacting with Co site at different spin states; **d** amounts of HCOOH, CO, and CH_4 produced. Reproduced with permission from Ref. [92]. Copyright 2020, American Chemical Society. **e** Proposed catalytic mechanism of Re-COF for CO_2 Reduction; **f** FTIR of COF, Re-COF and their starting materials; **g** amount of CO produced as a function of time, where top left inset shows zoomed in profile in the first 2-h reaction, and lower right inset shows recyclability of system after three 3-h experiments. Reproduced with permission from Ref. [93]. Copyright 2018, American Chemical Society

electrochemical reactions [91]. According to recent studies, photocatalytic performance is directly related to the intrinsic spin structure as well as the electronic structure of transition metals. Gong et al. [92] developed a strategy to

manipulate the spin state of cobalt on COFs (5,10,15,20-tetra(4-nitrophenyl)porphyrin as a metal-containing ligand) by varying oxidation states of porphyrin-centered, resulting in favorable activity and significantly enhanced selectivity

to HCOOH. Different spin states caused different degrees of coupling between the Co-3d_{xz} or Co-3d_{yz} orbital and the O-2p orbital, which affected the type of catalytic product and the catalytic rate (Fig. 3a, b). COF-367-CoIII demonstrates enhanced HCOOH production of (7.44 ± 0.37) µmol $((93.00 \pm 4.63)$ µmol·g^{-1}·h^{-1}), whereas reduced CO and CH$_4$ production of (0.44 ± 0.07) and (0.81 ± 0.09) µmol $((5.5 \pm 0.88)$ and (10.10 ± 1.12) µmol·g^{-1}·h^{-1}), respectively (Fig. 3d). This study explains the effect of the electronic structure of the transition metal central site on CO$_2$RR from the perspective of the spin state and demonstrates that the product species can be changed by modulating the state of the metal center.

Yang et al. [93] reported a newly designed 2D COF with incorporated Re complex synthesized from 4,4',4''-(1,3,5-triazine-2,4,6-triyl)trianiline and 2,2-bipyridyl-5,5-dialdehyde as ligands. This complex exhibited intrinsic light absorption and charge separation properties (Fig. 3e). The design of different monomers and the addition of Re atoms can effectively enhance the light absorption capacity (Fig. 3f). The recycling experiments present a good catalytic stability after reaction (Fig. 3h). This top-down approach to the preparation of Re containing MCOFs opens the door to a new generation of photovoltaic single-atom catalysts, but the long-term stability issues and deactivation mechanisms are still worthy of further investigation by researchers.

Liu et al. [94] developed a scalable general bottom-up approach for the facile synthesis of ultrathin (100 mg) and high yield (> 55%) COF-367 nanosheets via an imine exchange synthesis strategy by adding a large excess of 2,4,6-trimethylbenzaldehyde to the reaction system under solvothermal conditions. In particular, the isolated ultrathin COF-367-Co NSs displayed excellent efficiency with CO production rates up to 10,162 µmol·g^{-1}·h^{-1} under visible light irradiation and selectivity of $\sim$ 78% in aqueous media. This article exemplified the positive role of two-dimensional ultra-thin MCOFs materials in photocatalysis. Additional covalent organic frameworks (MP-TPE-COF, where M = H$_2$, Co and Ni; TPE = 4,4',4'',4'''-(ethane-1,1,2,2-tetramethyl) tetrabenzaldehyde) based on porphyrins-tetraphenyl have been reported as catalysts for efficient photocatalytic CO$_2$RR. Metalloporphyrin units play a key role in the selective adsorption, activation, and conversion of CO$_2$ as well as in the separation and electron transfer of charge carriers, allowing flexible modulation of photocatalytic activity and selectivity [95].

The final step in the photocatalytic reaction is product desorption, where the reaction is terminated and the catalyst becomes "poisoned" if the intermediate products are not released from the catalyst surface in time. In addition, some studies have suggested that organic substances including solvents, reactants, and surfactants used in

catalyst preparation may leave carbonaceous residues in the final product and may break down into small molecules such as CO and CH$_4$ during photocatalysis, leading to an overestimation of catalytic activity, and such issues are even more important for MCOFs catalysts. Therefore, it is necessary to confirm that the measured product is indeed from CO$_2$ reduction, not the decomposition of carbonaceous residues. Isotopic ^{13}CO$_2$ labeling is an effective technique for verifying the origin of reduction products and has been used extensively in many studies [96, 97].

3.2 MCOFs-based photocatalyst for HER

Besides the portion of photocatalystic CO$_2$RR, MCOFs have recently gained increasing attention in photochemical H$_2$ evolution from water. Wang and his co-workers proposed the designed synthesis of four isostructural porphyrinic two-dimensional covalent organic frameworks (MPor-DETH-COF, M = H$_2$, Co, Ni, Zn) for photocatalytic hydrogen generation [98]. The results presented that all four MCOFs adopt AA stacking structures with high crystallinity and large surface area. The detailed experiments and calculations showed that the four COFs have different excited-state charge separation capabilities, and the change trend of their separation capabilities was also keeping in line with the results of the photocatalytic hydrogen production experiment (CoPor-DETH-COF < H2Por-DETH-COF < NiPor-DETH-COF < ZnPor-DETH-COF). Interestingly, the incorporation of different transition metals into the porphyrin rings can rationally tune the photocatalytic hydrogen evolution rate of corresponding covalent organic frameworks. This tunable performance can be mainly explained by their tailored charge-carrier dynamics via molecular engineering. Zhao et al. [99] designed and synthesized a COF-based cocatalyst consisting of Pt and robust COFs, of which the robust COFs were based on electric donor-acceptor moieties. The electron-donor group of pyrene can be used for harvesting light and benzothiadiazole with different functional groups which can be as an electron acceptor to tune the light-adsorption ability of COFs. The highly ordered layered structure ensures that sufficient active sites are accessible for H$_2$ production and the donor-acceptor design can promote the separation of photogenerated carriers. In previous reports, a special structure of MCOF was developed and Lan's team successfully integrated two-dimensional COF with stable MOF [100]. By covalent lyan choring NH$_2$-UiO-66 onto the surface of TpPa-1-COF, a new type of MOF/COF hybrid stuff was synthesized. NH$_2$-UiO-66/TpPa-1-COF (4:6) showed the maximum photocatalytic H$_2$ evolution rate of 23.41 mmol·g^{-1}·h^{-1} (with the TOF of 402.36 h^{-1}), which was approximately 20 times higher

than that of the parent TpPa-1-COF, showing excellent light absorbance ability.

4 Applications in electrocatalyst

4.1 MCOFs-based electrocatalyst for CO_2RR

In recent years, many researches on the electrocatalytic reduction of CO_2 have appeared, promoting the rapid development of this field. Metals and metal oxide nanoparticles (such as Au, Pd, CuO_x, CoO_x) can catalyze the electrochemical reduction process of CO_2, then another point of concern is about the complexity of the product [101–103]. Considering the diversity of the valence states of the C element, it is possible to obtain a wide variety of products after CO_2 is reduced, such as CO, HCOOH, CH_4, C_xH_y, CH_3OH, C_2H_5OH, etc. [104, 105]. In short, the product depends on the number of electrons obtained by the CO_2 molecule and whether a C–C coupling reaction occurs. Although the technical routes of the two strategies of CO_2 electrocatalytic reduction and photocatalytic reduction are different, their essence is the same, that is, how to activate the inert CO_2 molecules and promote their reduction and conversion [97, 106]. In addition, the electron transfer and CO_2 activation process of the photocatalytic process is essentially an electrochemical process and can be enhanced by appropriate promoters (Fig. 4a).

In the past few years, copper-based electrocatalysts have received a lot of attention. On the one hand, CO_2RR shows higher reactivity on copper surface; on the other hand, some high-value C–C coupling products, such as C_2H_4, C_2H_6, will be found in its products. This is exemplified in the work by Ma et al. [107], in which copper-based catalysts within covalent triazine framework (CTF-B) were developed and it selectively performed CO_2RR on hydrocarbons with maximum faradaic efficiency (FE) of 81.3% and an FE of up to 30.6% for C_2H_4. It is proposed that the C–C coupling reaction was accelerated due to the increased CO coverage and enhanced local pH in the CO-saturated electrolyte, thus enhancing its reaction selectivity. Wu et al. [108] presented a tetrathiafulvalene (TTF) strut which was integrated into a two-dimensional cobalt porphyrin-based COF (TTF-Por(Co)-COF, 5,10,15,20-tetrakis (p-nitrophenyl)-21H and 23 h-porphyrin (TNPP) as ligands) to enhance its electron-transfer capability from the TTF to the porphyrin ring, resulting in enhanced CO_2RR performance in water with 95% Faradaic efficiency of the CO_2-to-CO conversion at −0.7 V (vs. RHE) and a partial current density of 6.88 mA·cm^{-2} at −0.9 V (vs. RHE). Cheung et al. [109] proposed the COF containing 5, 10, 15, 20-tetra-(4-aminophenyl)- porphyrin Fe(III) chloride (FeTAPPCl) and 2,5-dihydroxyterephthalaldehyde (Dha)

for the reduction of CO_2 to CO, which exhibited a good turnover frequency (> 600 h^{-1}·mol^{-1}) and reasonable faradaic efficiency for CO (an average of 80%) at −2.2 V (vs. Ag/AgCl) (Fig. 4b–d).

A stable and conductive COF (the phenazine-linked metallophthalocyanine CoPc-PDQ-COF) was developed by Huang et al. [110]. The CoPc-PDQ-COF are topologically connected via robust phenazine linkage into a two-dimensional tetragonal framework which is stable under various conditions (little weight loss (< 4 wt%)), including dimethylformamide (DMF), dimethyl sulfoxide (DMSO), tetrahydrofuran (THF), methanol (MeOH), cyclohexane, water (100 and 258 °C), concentrated HCl (12 mol·L^{-1}), and NaOH solution (14 mol·L^{-1}) (Fig. 4e). With stable structure and Co active site, the electrocatalytic framework exhibits a faradaic efficiency of 96%, an exceptional turnover number up to 320,000, and a long-term turnover frequency of 11,412 h^{-1}, which is a 32-fold improvement over molecular catalyst (Fig. 4f, g).

The specificity of the reaction yield is one of the important concerns and most studies have difficulty in proposing universal guidelines, so this is a great challenge for complex electrocatalytic processes. The design of electrocatalytic materials for CO_2-reduced MCOFs has mostly focused on Co- and Cu-based porphyrin COFs and much effort has been spent on the structural optimization of the catalytic sites and possible reaction pathways, which are important for the overall catalytic performance but not ideal due to the limitations of the optimization methods. Whereas Cui's team reported the double-layer hydrophobic nanoporous Au/PE membrane, a biomimetic and efficient artificial alveolar structure for CO_2RR [111]. The interconnected nanopores of the hydrophobic polyethylene membrane enable efficient CO_2 transport at high flux but inhibit water permeation, further enhancing the electrocatalytic CO_2RR through local pH increase while inhibiting the reduction of H_2O. This artificial alveolar design maximizes the efficiency of the three-phase contact, resulting in excellent CO_2 reduction activity even at low catalyst loadings. Liang et al. [112] systematically investigated the effect of hydrophobicity on the production of ethylene from CO_2RR by coating the CuO electrocatalyst surface with different polymers. Polyvinyl alcohol and polyvinylpyrrolidone modified copper nanoparticles were more favorable to hydrogen precipitation reactions. These advanced reports demonstrated the importance of the microenvironment for CO_2RR, and the design ideas presented are relevant for the embodiment of MCOFs. While designing the reactivity, we need to be aware of the importance of the three interfaces for the reduction of carbon dioxide.
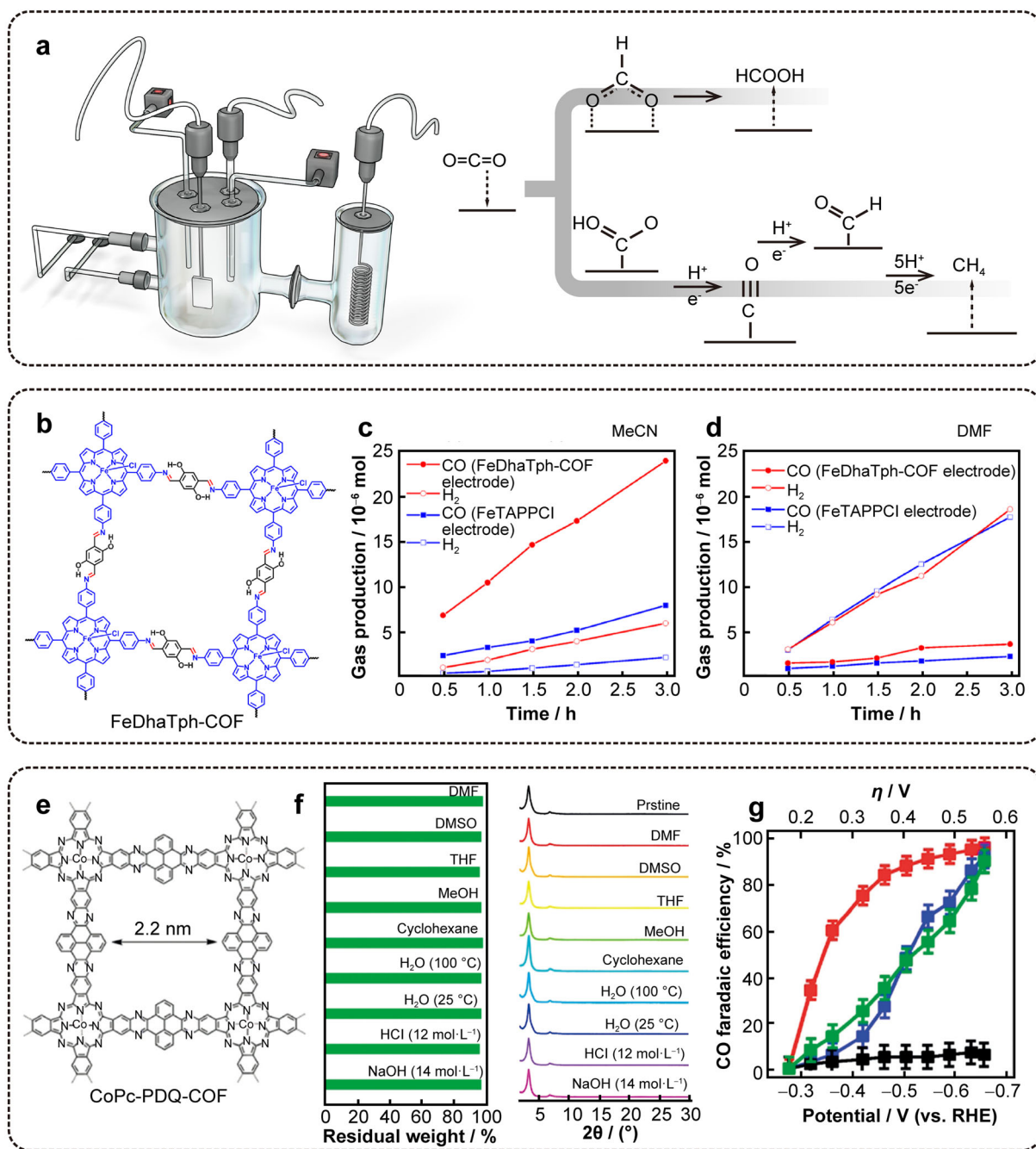
Fig. 4 a Schematic diagram of electrocatalytic CO_2RR system and corresponding reduction process; b proposed structure of FeDhaTph-COF; number of moles of CO and H_2 (red for FeDhaTph-COF electrode and blue for FeTAPPCl electrode) in 3-h CPE in c MeCN and d DMF. Reproduced with permission from Ref. [109]. Copyright 2019, American Chemical Society. e Proposed structure of CoPc-PDQ-COF and f chemical stability; g faradaic efficiencies of CoPc-PDQ-COF (red curve), monomeric $[NH_2]_8$CoPc (blue curve), commercial CoPc (green curve), and carbon fiber (black curve). Reproduced with permission from Ref. [110]. Copyright 2020, WILEY–VCH

4.2 MCOFs-based electrocatalyst for OER/ORR/ HER

Noble-metal-free electrocatalysts for highly efficient oxygen reduction reaction (ORR), oxygen evolution reaction (OER), and hydrogen evolution reaction (HER) are highly demanded in energy conversion and storage techniques due to its high energy density and low cost. The rotating disk electrode (RDE) technique is often used as a test system to evaluate the above three reactions, which is a powerful tool to rapidly evaluate the activity and reaction pathways of oxygen reactions (Fig. 5a) [113, 114]. The ORR is a typical
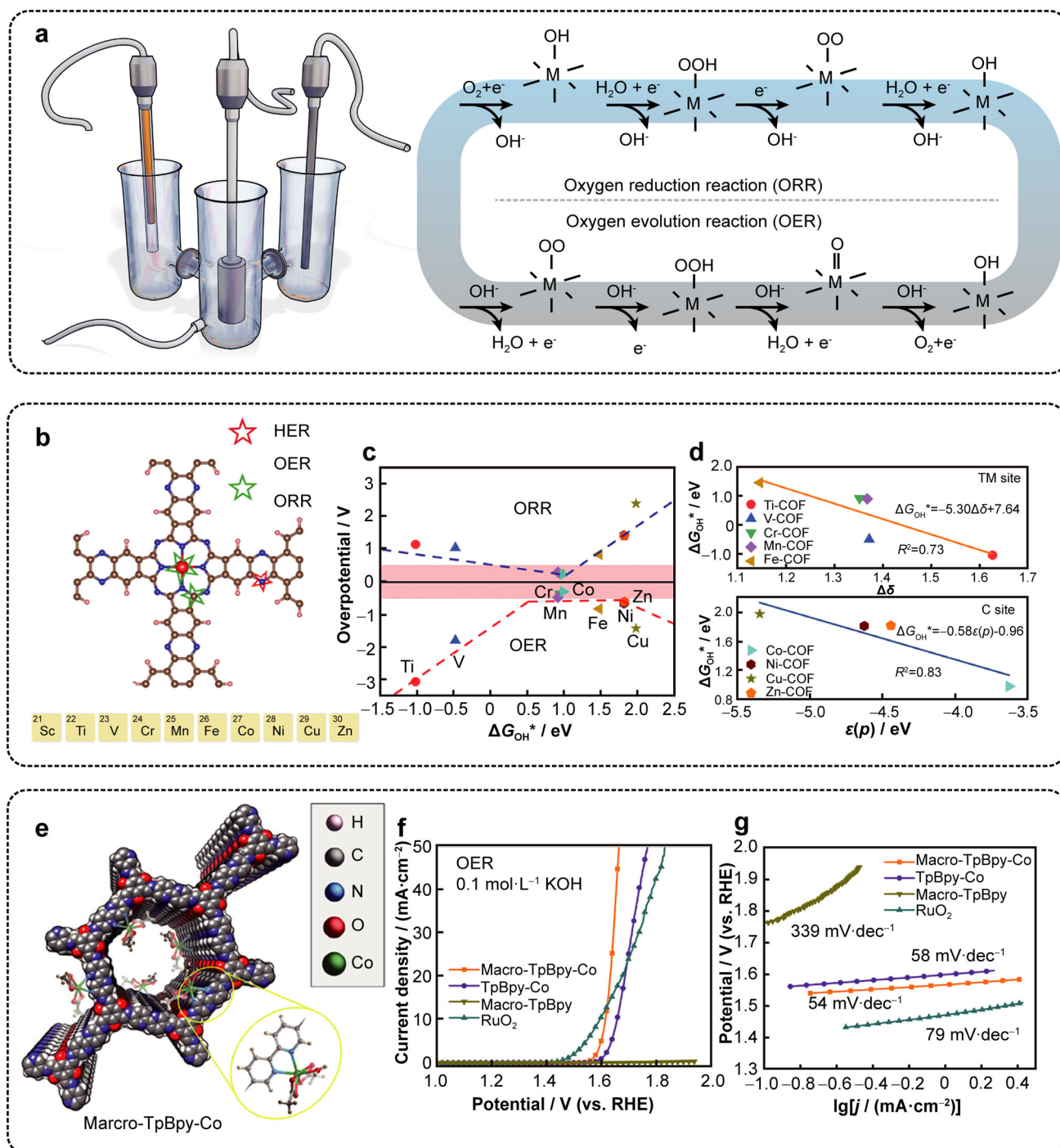
Fig. 5 **a** Electrocatalytic three-electrode system for OER, ORR and HER and corresponding ORR and OER reaction process; **b** three plausible active sites considered labeled by stars of different colors, where red represents HER site and green denotes OER/ORR sites; **c** dual volcano plot for ORR and OER on TM-COF monolayers, where points represent a calculated overpotential for each system as a function of OH* binding energy; **d** linear relationships between Gibbs free energy and transition-metal electron transfer ($\Delta\delta$) for TM sites (top panel) or Gibbs free energy and p-band center position for C sites (bottom panel). Reproduced with permission from Ref. [126]. Copyright 2020, American Chemical Society. **e** Schematic representation of synthesis of macro-TpBpy-Co; **f** OER performance of macro-COF-Co and **g** corresponding Tafel plots. Reproduced with permission from Ref. [127]. Copyright 2019, American Chemical Society

structure-sensitive reaction ($4e^- + 4H^+$ (aq) $+ O_2$ (g) $\rightarrow 2H_2O$). Its pathways and mechanisms depend on

coordination environment and electronic structure of active site [115]. The active site interacts with O_2 adsorbed on the

oxide surface in the form of end-on or side-on, and the strength of the oxygen-related adsorption structure and active sites depends on the microstructure and binding energy. The electrolysis of water involves two half-cell reactions: the hydrogen evolution reaction (HER, $2H^+$ (aq) $+ 2e^- \rightarrow H_2$ (g)) and the oxygen evolution reaction (OER, $2H_2O$ (l) $\rightarrow 4e^- + 4H^+$ (aq) $+ O_2$ (g)) [116–120]. OER and ORR are a pair of opposite reactions, and the corresponding bifunctional oxygen catalyst has higher requirements for the mass transfer structure [121]. Like any other chemical reaction, energy input is required to overcome the barrier in electrochemical processes to produce corresponding product. ORR, OER, and HER all require suitable catalysts to minimize the consumption for energy conversion [122–125]. Scientific and effective design is meaningful and challenging for MCOFs electrocatalyst.

Wang et al. [126] demonstrated that the two-dimensional COFs of phthalocyanines and pyrazine linkages can firmly anchor transition-metal (TM) atoms. The resultant TM embedded COFs (TM-COFs) exhibited multifunctional electrocatalytic activity for HER, OER, and ORR, which can be attributed to the synergistic effect of the anchored TM atoms and COFs. Among the series of metal-COFs, Mn, Cr-COFs are predicted to have extremely low overpotentials of $-0.014/0.44/0.31$ and $-0.239/0.35/0.29$ V for HER/OER/ORR, respectively (Fig. 5b, c). This research also proposed that the degree of electron transfer from TM atom to the framework ($\Delta\delta$) and p-band center (ε_p) of carbon atoms can act as descriptors for the adsorption strength of intermediates on the TM-COF monolayers. The new descriptors offer useful guidance for the experimental design of advanced-efficiency OER/ORR/HER catalysts. At the same time, this review also conveys an important message, that is, as an electrocatalyst, metal-COFs have great potential in theory (Fig. 5d).

Another valuable theory-related literature pointed out that optimal ORR catalysts should have moderate binding strength (ΔE_{ads}) with O_2-derived intermediates, where the metal species and its coordination numbers are the essential determining factors for ΔE_{ads}. Iwase et al. [22] proposed a monotonic increase in the adsorption intensity of intermediates with d-electron number or metal center coordination number decreasing and observed a volcano-shaped relationship between the adsorption energy of intermediates and the theoretical ORR activity. Undoubtedly, the metal-COFs have strong oxygen catalytic activity and hydrogen evolution activity due to its flexible controllable active site. However, the requirements for excellent electrocatalysts go far beyond this, fast mass transport and high conductivity are also required. Zhao et al. [127] introduced a bipyridine group into the COF backbone, where metals such as CO_2^+ can be coordinated within a layered pore structure, to prepare a new OER catalyst (macro-TpBpy-Co) with a

unique pore structure, which is a great improvement over pure microporous COF and competes for an overpotential of 380 mV at 10 mA·cm^{-2} (Fig. 5e–g), attributing to the improved mass diffusion properties in the layered porous COF structure and easy access to the active CO_2^+-bipyridine sites.

For some applications, especially where fast mass transfer is required, a layered pore structure is an ideal solution. For example, small micropores can provide a larger surface area, while large pores can provide unhindered transportation on the surface of the material. The subsequent pyrolysis is often needed due to their poor intrinsic electrical conductivity, leading to undesirable structure changes and destruction of the original fine structure. An effective method is to combine MCOFs with a good conductive substrate. Guo et al. [128] designed hybrid electrocatalysts consist of self-assembling pristine COP with reduced graphene oxide (rGO). The electrical conductivity of the hybridized COP/rGO materials is increased by more than seven orders of magnitude (from 3.06×10^{-9} to 2.56×10^{-1} S·m^{-1}) compared with that of pure COPs. The ORR activities of the hybrid are enhanced significantly by the synergetic effect between highly active COP and highly conductive rGO. This COP/rGO hybrid catalyst exhibited a remarkable positive half-wave (150 mV).

In addition to the aforementioned MCOF catalysts incorporating metal-containing monomers, MCOFs prepared from the top-down method can also have excellent catalytic performance, Park et al. [129] developed well-dispersed and highly stable platinum nanoparticles (PtNPs) supported on a covalent organic framework (COF-bpyTPP), which shows superior catalytic performance compared to the commercially available Pt/C under the same alkaline conditions, producing 13 times more hydrogen with a far more positive onset potential (-0.13 V vs. -0.63 V) and ca. 100% faradaic efficiency. As clearly elaborated, by controlling and optimizing key factors such as microstructure and load transfer efficiency, MCOFs with its unique electronic structure can be processed into an excellent ORR/OER/HER catalyst.

5 Summary and prospect

5.1 Conclusion

In this article, we summarized some recent advances in the MCOFs catalyst from the perspective of the design principles, construction strategies, and structure–property relationships. From all aspects, the composites, or derivatives of MCOFs can facilitate the reaction kinetics and present enhanced cycling capacity due to their good

conductivity, rigid frameworks, and abundant active sites. Despite some serious problems and challenges, there is no doubt that MCOFs-based catalysts have great potential to flourish as sustainable photo/electrocatalysts, and the implementation of MCOFs into new conversion systems, such as "coupled energy conversion technologies" and "membrane reactors", will be successful in the future work. And more favorable substitution of organic upgrading reactions or accelerating of multi-stimulus coupling will be sure to offer possibilities for efficient energy conversion technologies [130–132].

5.2 Perspective and challenges

The study of micromorphology of catalysts has been one of the hot topics of research. The hollow or porous 3D structures, of which the artificial morphology can expose more surfaces, improve the mass transfer rate and optimize the adsorption of catalysts with ORR intermediates by regulating the surface stress and coordination [133]. In addition, the construction of one-dimensional nanostructures can prevent the agglomeration of catalysts, then expose the active sites and prevent the degeneration of activity [121, 134, 135]. However, few studies have been focused on the control of morphology of MCOFs due to the rise from the fixed nature of the COFs and the limitations of the synthesis method. Wang et al. [136] proposed reversible polycondensation-termination (RPT) polymerization method, which can be used to customize a variety of 2D COF materials with high crystallinity and regular morphology. For imine COF systems, some researchers proposed that aniline and benzaldehyde can be used as competing agents to reversibly restrict the amino and aldehyde groups in the condensate for achieving a reversible switch between the terminated and active states of the polymerization groups and freeing the reaction system from kinetic traps to achieve thermodynamic control. Three kinds of things can be developed from this polymerization, that is, morphologies-microspheres, hollow microfibers, and thin films, and all of them are made of two-dimensional COF nanosheets stacked. A COF film was grown on the inner wall of a micron copper tube for loading palladium nanoparticles to construct a loaded microreactor, which could complete the reduction of p-nitropheno with an average residence time of only 3.2 s. The TOF was 1–2 orders of magnitude higher compared to the powder COF-loaded catalyst. The design idea also can be extended to photo/electrochemical MCOFs catalytic systems to exploit the potential catalytic efficiency of MCOFs through morphology modulation. Moreover, Fe_3O_4 nanoclusters are encapsulated by mixed-order polyimide lattice structures through Schiff base reaction, and the formed imine bonds, controlled thermodynamically, transform from polyimide lattice structures to crystalline COFs. Such core–shell nanospheres with the characteristics of uniform size, spherical shape, and controllable shell wall thickness exhibit unique photothermal properties in the near-infrared region [137].

Among the more promising applications of MCOFs, technologies such as fuel cells and separation processes place new demands on performance. The microscopic morphology of MCOFs determines to some extent their catalytic performance, while their membrane-forming properties greatly influence the feasibility of practical applications, which can integrate MCOFs into advanced energy conversion systems at a lower cost. High selectivity and high permeability are two essential characteristics of an ideal membrane. However, the fabrication of MCOFs membranes remains a great challenge and the main obstacle to achieve this goal is the inherent properties of MCOFs and the complexity of the membrane preparation process. Conventional COF membrane synthesis is mainly by situ solvent heat, self-assembly, and interfacial polymerization, but for now, at least, large-scale preparation of thin COF membranes with good mechanical property is difficult to achieve; therefore, one of the important breakthrough points in the development of MCOFs is the optimization of membrane engineering [138–140].

In terms of the structural design of MCOFs, the molecular design of "knots" and "links" is still of great importance for photo/electrocatalysis and most MCOFs use porphyrin-based monomers as structural units, so its singularity of the functional structure limits the performance. In recent years, with the development of synthetic methods, characterization techniques, catalytic mechanisms, and theoretical studies of single-atom catalysts, impressive research results have been presented. A new concept called polyatomic catalyst has been proposed by researchers, which not only means doubling the functionality of individual atoms but also gives the possibility to surpass the theoretical performance limit by its synergistic effect [141, 142]. An advanced study showed that the broken ligand-field symmetry is the key for active CO_2 electrolysis in Ni-containing porphyrin monomers because it subordinates an increase in the Ni redox potential and yield Ni^I. Certainly, this important discovery breaks the general concept of porphyrin-based COF catalysts [143]. In addition, the modulation of properties is not limited to the design of metal-containing structural units, and the research of organic skeletons is also worthy of attention. Wei et al. [144] developed a C3-symmetric benzotrithiophene tricarbaldehyde (BTT) based COF. Their study proposed that the construction of monomers with ratios of sp^2 carbon facilitates the charge transfer effect and indicates that dealing with COFs of designated structures under ionothermal condition is a great method to build highly

conductive structure-controllable materials for electrochemical applications. The bottom-up design idea has been promoted due to its design flexibility as well as theoretical feasibility. In the design of MCOFs-based photo/electrocatalysts, it should not only consider about the catalytic benefits of the active building block but also enhance the overall structural performance from the perspective of electrical conductivity.

Declarations

Conflict of interests The authors declare that they have no conflict of interest.

References

[1] Chandrasekaran S, Yao L, Deng L, Bowen C, Zhang Y, Chen S, Lin Z, Peng F, Zhang P. Recent advances in metal sulfides: from controlled fabrication to electrocatalytic, photocatalytic and photoelectrochemical water splitting and beyond. Chem Soc Rev. 2019;48(15):4178.

[2] Zhu JY, Liang F, Yao YC, Ma WH, Yang B. Preparation and application of metal organic frameworks derivatives in electro-catalysis. Chin J Rare Met. 2019;43(2):186.

[3] Gao H, Yue HH, Qi F, Yu B, Zhang WL, Chen YF. Few-layered ReS_2 nanosheets grown on graphene as electrocatalyst for hydrogen evolution reaction. Rare Met. 2018; 37(12):1014.

[4] Duan X, Xu J, Wei Z, Ma J, Guo S, Wang S, Liu H, Dou S. Metal-free carbon materials for CO_2 electrochemical reduction. Adv Mater. 2017;29(41):1701784.

[5] Gonglach S, Paul S, Haas M, Pillwein F, Sreejith SS, Barman S, De R, Mullegger S, Gerschel P, Apfel UP, Coskun H, Aljabour A, Stadler P, Schofberger W, Roy S. Molecular cobalt corrole complex for the heterogeneous electrocatalytic reduction of carbon dioxide. Nat Commun. 2019;10:3864.

[6] Ju W, Bagger A, Hao GP, Varela AS, Sinev I, Bon V, Roldan Cuenya B, Kaskel S, Rossmeisl J, Strasser P. Understanding activity and selectivity of metal-nitrogen-doped carbon catalysts for electrochemical reduction of CO_2. Nat Commun. 2017;8:944.

[7] Ahn SH, Yu X, Manthiram A. "Wiring" Fe-N_x -embedded porous carbon framework onto 1d nanotubes for efficient oxygen reduction reaction in alkaline and acidic media. Adv Mater. 2017;29(26):1606534.

[8] Cheng WZ, Liang JL, Yin HB, Wang YJ, Yan WF, Zhang JN. Bifunctional iron-phtalocyanine metal–organic framework catalyst for ORR, OER and rechargeable zinc–air battery. Rare Met. 2020;39(7):815.

[9] Del Carmen GL, Kurtoglu A, Walsh DA, Khlobystov AN. Extremely stable platinum-amorphous carbon electrocatalyst within hollow graphitized carbon nanofibers for the oxygen reduction reaction. Adv Mater. 2016;28(41):9103.

[10] Kim C, Dionigi F, Beermann V, Wang X, Moller T, Strasser P. Alloy nanocatalysts for the electrochemical oxygen reduction (ORR) and the direct electrochemical carbon dioxide reduction reaction (CO_2RR). Adv Mater. 2019;31(31):1805617.

[11] Qian Q, Asinger PA, Lee MJ, Han G, Mizrahi Rodriguez K, Lin S, Benedetti FM, Wu AX, Chi WS, Smith ZP. MOF-based membranes for gas separations. Chem Rev. 2020;120(16): 8161.

[12] Wang Q, Astruc D. State of the art and prospects in metal-organic framework (MOF)-based and MOF-derived nanocatalysis. Chem Rev. 2020;120(2):1438.

[13] Bavykina A, Kolobov N, Khan IS, Bau JA, Ramirez A, Gascon J. Metal-organic frameworks in heterogeneous catalysis: recent progress, new trends, and future perspectives. Chem Rev. 2020; 120(16):8468.

[14] Ding SY, Wang W. Covalent organic frameworks (COFs): from design to applications. Chem Soc Rev. 2013;42(2):548.

[15] Evans AM, Bradshaw NP, Litchfield B, Strauss MJ, Seckman B, Ryder MR, Castano I, Gilmore C, Gianneschi NC, Mulzer CR, Hersam MC, Dichtel WR. High-sensitivity acoustic molecular sensors based on large-area, spray-coated 2D covalent organic frameworks. Adv Mater. 2020;32(42):2004205.

[16] Feng X, Chen L, Honsho Y, Saengsawang O, Liu L, Wang L, Saeki A, Irle S, Seki S, Dong Y, Jiang D. An ambipolar conducting covalent organic framework with self-sorted and periodic electron donor-acceptor ordering. Adv Mater. 2012; 24(22):3026.

[17] Feriante CH, Jhulki S, Evans AM, Dasari RR, Slicker K, Dichtel WR, Marder SR. Rapid synthesis of high surface area imine-linked 2D covalent organic frameworks by avoiding pore collapse during isolation. Adv Mater. 2020;32(2): 1905776.

[18] Guan X, Chen F, Fang Q, Qiu S. Design and applications of three dimensional covalent organic frameworks. Chem Soc Rev. 2020;49(5):1357.

[19] Hou J, Zhang H, Simon GP, Wang H. Polycrystalline advanced microporous framework membranes for efficient separation of small molecules and ions. Adv Mater. 2020;32(18):1902009.

[20] Qin Y, Wan Y, Guo J, Zhao M. Two-dimensional metal-organic framework nanosheet composites: preparations and applications. Chin Chem Lett. 2021. https://doi.org/10.1016/j.cclet.2021.07.013.

[21] Chen W, Pei J, He CT, Wan J, Ren H, Wang Y, Dong J, Wu K, Cheong WC, Mao J, Zheng X, Yan W, Zhuang Z, Chen C, Peng Q, Wang D, Li Y. Single tungsten atoms supported on MOF-derived N-doped carbon for robust electrochemical hydrogen evolution. Adv Mater. 2018;30(30):1800396.

[22] Iwase K, Nakanishi S, Miyayama M, Kamiya K. Rational molecular design of electrocatalysts based on single-atom modified covalent organic frameworks for efficient oxygen reduction reaction. ACS Appl Energ Mater. 2020;3(2):1644.

[23] Joshi T, Chen C, Li H, Diercks CS, Wang G, Waller PJ, Li H, Bredas JL, Yaghi OM, Crommie MF. Local electronic structure of molecular heterojunctions in a single-layer 2D covalent organic framework. Adv Mater. 2019;31(3):1805941.

[24] Keller N, Bein T. Optoelectronic processes in covalent organic frameworks. Chem Soc Rev. 2021;50(3):1813.

[25] Kong L, Zhong M, Shuang W, Xu Y, Bu XH. Electrochemically active sites inside crystalline porous materials for energy storage and conversion. Chem Soc Rev. 2020;49(8):2378.

[26] Li J, Jing X, Li Q, Li S, Gao X, Feng X, Wang B. Bulk COFs and COF nanosheets for electrochemical energy storage and conversion. Chem Soc Rev. 2020;49(11):3565.

[27] Lin CY, Zhang D, Zhao Z, Xia Z. Covalent organic framework electrocatalysts for clean energy conversion. Adv Mater. 2018; 30(5):1703646.

[28] Liu X, Huang D, Lai C, Zeng G, Qin L, Wang H, Yi H, Li B, Liu S, Zhang M, Deng R, Fu Y, Li L, Xue W, Chen S. Recent

advances in covalent organic frameworks (COFs) as a smart sensing material. Chem Soc Rev. 2019;48(20):5266.

[29] Grimaud A, Demortière A, Saubanère M, Dachraoui W, Duchamp M, Doublet ML, Tarascon JM. Activation of surface oxygen sites on an iridium-based model catalyst for the oxygen evolution reaction. Nat Energy. 2016;2(2):16189.

[30] Grimaud A, Diaz-Morales O, Han B, Hong WT, Lee YL, Giordano L, Stoerzinger KA, Koper MTM, Shao-Horn Y. Activating lattice oxygen redox reactions in metal oxides to catalyse oxygen evolution. Nat Chem. 2017;9(5):457.

[31] Jiang K, Luo M, Peng M, Yu Y, Lu YR, Chan TS, Liu P, de Groot FMF, Tan Y. Dynamic active-site generation of atomic iridium stabilized on nanoporous metal phosphides for water oxidation. Nat Commun. 2020;11(1):2701.

[32] Rotondi S, Tartaglione L, Muci ML, Farcomeni A, Pasquali M, Mazzaferro S. Oxygen extraction ratio (OER) as a measurement of hemodialysis (HD) induced tissue hypoxia: a pilot study. Sci Rep. 2018;8:5655.

[33] Liu C, Dong H, Ji Y, Hou T, Li Y. Origin of the catalytic activity of phosphorus doped MoS_2 for oxygen reduction reaction (ORR) in alkaline solution: a theoretical study. Sci Rep. 2018;8:13292.

[34] Lu Z, Xu W, Ma J, Li Y, Sun X, Jiang L. Superaerophilic carbon-nanotube-array electrode for high-performance oxygen reduction reaction. Adv Mater. 2016;28(33):7155.

[35] Mun Y, Lee S, Kim K, Kim S, Lee S, Han JW, Lee J. Versatile strategy for tuning ORR activity of a single Fe-N_4 site by controlling electron-withdrawing/donating properties of a carbon plane. J Am Chem Soc. 2019;141(15):6254.

[36] Park SA, Lee EK, Song H, Kim YT. Bifunctional enhancement of oxygen reduction reaction activity on Ag catalysts due to water activation on $LaMnO_3$ supports in alkaline media. Sci Rep. 2015;5:13552.

[37] Puangsombut P, Tantavichet N. Effect of plating bath composition on chemical composition and oxygen reduction reaction activity of electrodeposited Pt–Co catalysts. Rare Met. 2019;38(2):95.

[38] Bi S, Yang C, Zhang W, Xu J, Liu L, Wu D, Wang X, Han Y, Liang Q, Zhang F. Two-dimensional semiconducting covalent organic frameworks via condensation at arylmethyl carbon atoms. Nat Commun. 2019;10:2467.

[39] Biswal BP, Valligatla S, Wang M, Banerjee T, Saad NA, Mariserla BMK, Chandrasekhar N, Becker D, Addicoat M, Senkovska I, Berger R, Rao DN, Kaskel S, Feng X. Nonlinear optical switching in regioregular porphyrin covalent organic frameworks. Angew Chem Int Ed. 2019;58(21):6896.

[40] Chen R, Shi JL, Ma Y, Lin G, Lang X, Wang C. Designed synthesis of a 2D porphyrin-based sp^2 carbon-conjugated covalent organic framework for heterogeneous photocatalysis. Angew Chem Int Ed. 2019;58(19):6430.

[41] Derevyannikova EA, Kardash TY, Stadnichenko AI, Stonkus OA, Slavinskaya EM, Svetlichnyi VA, Boronin AI. Structural insight into strong Pt–CeO_2 interaction: from single Pt atoms to PtO_x clusters. J Phys Chem C. 2018;123(2):1320.

[42] Hao W, Chen D, Li Y, Yang Z, Xing G, Li J, Chen L. Facile synthesis of porphyrin based covalent organic frameworks via an A_2B_2 monomer for highly efficient heterogeneous catalysis. Chem Mater. 2019;31(19):8100.

[43] Jin E, Lan Z, Jiang Q, Geng K, Li G, Wang X, Jiang D. 2D sp^2 carbon-conjugated covalent organic frameworks for photocatalytic hydrogen production from water. Chem. 2019;5(6):1632.

[44] Kuznetsov DA, Chen Z, Kumar PV, Tsoukalou A, Kierzkowska A, Abdala PM, Safonova OV, Fedorov A, Muller CR. Single site cobalt substitution in 2D molybdenum carbide (mxene) enhances catalytic activity in the hydrogen evolution reaction. J Am Chem Soc. 2019;141(44):17809.

[45] Peng X, Zhao S, Mi Y, Han L, Liu X, Qi D, Sun J, Liu Y, Bao H, Zhuo L, Xin HL, Luo J, Sun X. Trifunctional single-atomic Ru sites enable efficient overall water splitting and oxygen reduction in acidic media. Small. 2020;16(33):2002888.

[46] Shi JL, Chen R, Hao H, Wang C, Lang X. 2D sp^2 carbon-conjugated porphyrin covalent organic framework for cooperative photocatalysis with tempo. Angew Chem Int Ed. 2020;59(23):9088.

[47] Sun M, Ji J, Hu M, Weng M, Zhang Y, Yu H, Tang J, Zheng J, Jiang Z, Pan F, Liang C, Lin Z. Overwhelming the performance of single atoms with atomic clusters for platinum-catalyzed hydrogen evolution. ACS Catal. 2019;9(9):8213.

[48] Xiao X, Gao Y, Zhang L, Zhang J, Zhang Q, Li Q, Bao H, Zhou J, Miao S, Chen N, Wang J, Jiang B, Tian C, Fu H. A promoted charge separation/transfer system from Cu single atoms and C_3N_4 layers for efficient photocatalysis. Adv Mater. 2020;32(33):2003082.

[49] Ye L, Ying Y, Sun D, Zhang Z, Fei L, Wen Z, Qiao J, Huang H. Highly efficient porous carbon electrocatalyst with controllable N-species content for selective CO_2 reduction. Angew Chem Int Ed. 2020;59(8):3244.

[50] Zhang H, Yu L, Chen T, Zhou W, Lou XWD. Surface modulation of hierarchical MoS_2 nanosheets by Ni single atoms for enhanced electrocatalytic hydrogen evolution. Adv Funct Mater. 2018;28(51):1807086.

[51] Chao Y, Zhou P, Li N, Lai J, Yang Y, Zhang Y, Tang Y, Yang W, Du Y, Su D, Tan Y, Guo S. Ultrathin visible-light-driven Mo incorporating In_2O_3 -$ZnIn_2Se_4$ z-scheme nanosheet photocatalysts. Adv Mater. 2019;31(5):1807226.

[52] Chu S, Ou P, Ghamari P, Vanka S, Zhou B, Shih I, Song J, Mi Z. Photoelectrochemical CO_2 reduction into syngas with the metal/oxide interface. J Am Chem Soc. 2018;140(25):7869.

[53] Ji X, Kang Y, Fan T, Xiong Q, Zhang S, Tao W, Zhang H. An antimonene/Cp*Rh(phen)Cl/black phosphorus hybrid nanosheet-based z-scheme artificial photosynthesis for enhanced photo/bio-catalytic CO_2 reduction. J Mater Chem A. 2020;8(1):323.

[54] Jin J, Yu J, Guo D, Cui C, Ho W. A hierarchical z-scheme CdS-WO_3 photocatalyst with enhanced CO_2 reduction activity. Small. 2015;11(39):5262.

[55] Jing L, Zhou J, Durrant JR, Tang J, Liu D, Fu H. Dynamics of photogenerated charges in the phosphate modified TiO_2 and the enhanced activity for photoelectrochemical water splitting. Energ Environ Sci. 2012;5(4):6552.

[56] Liang L, Lei F, Gao S, Sun Y, Jiao X, Wu J, Qamar S, Xie Y. Single unit cell bismuth tungstate layers realizing robust solar CO_2 reduction to methanol. Angew Chem Int Ed. 2015;54(47):13971.

[57] Liu Z, Wang L, Yu X, Zhang J, Yang R, Zhang X, Ji Y, Wu M, Deng L, Li L, Wang ZL. Piezoelectric-effect-enhanced full-spectrum photoelectrocatalysis in p–n heterojunction. Adv Funct Mater. 2019;29(41):1807279.

[58] Peng Y, Zhao M, Chen B, Zhang Z, Huang Y, Dai F, Lai Z, Cui X, Tan C, Zhang H. Hybridization of mofs and COFs: a new strategy for construction of MOF@COF core-shell hybrid materials. Adv Mater. 2018;30(3):1705454.

[59] Segura JL, Mancheno MJ, Zamora F. Covalent organic frameworks based on schiff-base chemistry: synthesis, properties and potential applications. Chem Soc Rev. 2016;45(20):5635.

[60] Meng L, Wang S, Cao F, Tian W, Long R, Li LL. Doping-induced amorphization, vacancy, and gradient energy band in SnS_2 nanosheet arrays for improved photoelectrochemical water splitting. Angew Chem Int Ed. 2019;58(20):6761.

[61] Pan Z, Zhang G, Wang X. Polymeric carbon nitride/reduced graphene oxide/Fe_2O_3: all-solid-state z-scheme system for

photocatalytic overall water splitting. Angew Chem Int Ed. 2019;58(21):7102.

[62] Ren H, Dittrich T, Ma H, Hart JN, Fengler S, Chen S, Li Y, Wang Y, Cao F, Schieda M, Ng YH, Xie Z, Bo X, Koshy P, Sheppard LR, Zhao C, Sorrell CC. Manipulation of charge transport by metallic $V_{13}O_{16}$ decorated on bismuth vanadate photoelectrochemical catalyst. Adv Mater. 2019;31(8):1807204.

[63] Wang JC, Yao HC, Fan ZY, Zhang L, Wang JS, Zang SQ, Li ZJ. Indirect z-scheme bioi/g-C_3N_4 photocatalysts with enhanced photoreduction CO_2 activity under visible light irradiation. ACS Appl Mater Interfaces. 2016;8(6):3765.

[64] Segura JL, Royuela S, Mar RM. Post-synthetic modification of covalent organic frameworks. Chem Soc Rev. 2019;48(14):3903.

[65] Zhang L, Han L, Liu H, Liu X, Luo J. Potential-cycling synthesis of single platinum atoms for efficient hydrogen evolution in neutral media. Angew Chem Int Ed. 2017;56(44):13694.

[66] Zhao Y, Liu H, Wu C, Zhang Z, Pan Q, Hu F, Wang R, Li P, Huang X, Li Z. Fully conjugated two-dimensional sp^2-carbon covalent organic frameworks as artificial photosystem with high efficiency. Angew Chem Int Ed. 2019;58(16):5376.

[67] Wang H, Zeng Z, Xu P, Li L, Zeng G, Xiao R, Tang Z, Huang D, Tang L, Lai C, Jiang D, Liu Y, Yi H, Qin L, Ye S, Ren X, Tang W. Recent progress in covalent organic framework thin films: fabrications, applications and perspectives. Chem Soc Rev. 2019;48(2):488.

[68] Yusran Y, Fang Q, Valtchev V. Electroactive covalent organic frameworks: design, synthesis, and applications. Adv Mater. 2020;32(44):2002038.

[69] Wang Z, Zhang S, Chen Y, Zhang Z, Ma S. Covalent organic frameworks for separation applications. Chem Soc Rev. 2020;49(3):708.

[70] Sun Q, Aguila B, Ma S. A bifunctional covalent organic framework as an efficient platform for cascade catalysis. Materials Chemistry Frontiers. 2017;1(7):1310.

[71] Sun Q, Aguila B, Perman J, Nguyen N, Ma S. Flexibility matters: cooperative active sites in covalent organic framework and threaded ionic polymer. J Am Chem Soc. 2016;138(48):15790.

[72] Wang P, Xu Q, Li Z, Jiang W, Jiang Q, Jiang D. Exceptional iodine capture in 2D covalent organic frameworks. Adv Mater. 2018;30:1801991.

[73] Aiyappa HB, Thote J, Shinde DB, Banerjee R, Kurungot S. Cobalt-modified covalent organic framework as a robust water oxidation electrocatalyst. Chem Mater. 2016;28(12):4375.

[74] Calik M, Auras F, Salonen LM, Bader K, Grill I, Handloser M, Medina DD, Dogru M, Lobermann F, Trauner D, Hartschuh A, Bein T. Extraction of photogenerated electrons and holes from a covalent organic framework integrated heterojunction. J Am Chem Soc. 2014;136(51):17802.

[75] Tavakoli E, Kakekhani A, Kaviani S, Tan P, Ghaleni MM, Zaeem MA, Rappe AM, Nejati S. In situ bottom-up synthesis of porphyrin-based covalent organic frameworks. J Am Chem Soc. 2019;141(50):19560.

[76] Diercks CS, Lin S, Kornienko N, Kapustin EA, Nichols EM, Zhu C, Zhao Y, Chang CJ, Yaghi OM. Reticular electronic tuning of porphyrin active sites in covalent organic frameworks for electrocatalytic carbon dioxide reduction. J Am Chem Soc. 2018;140(3):1116.

[77] Yusran Y, Li H, Guan X, Li D, Tang L, Xue M, Zhuang Z, Yan Y, Valtchev V, Qiu S, Fang Q. Exfoliated mesoporous 2D covalent organic frameworks for high-rate electrochemical double-layer capacitors. Adv Mater. 2020;32(8):1907289.

[78] Geng K, He T, Liu R, Dalapati S, Tan KT, Li Z, Tao S, Gong Y, Jiang Q, Jiang D. Covalent organic frameworks: design, synthesis, and functions. Chem Rev. 2020;120(16):8814.

[79] Zhong W, Sa R, Li L, He Y, Li L, Bi J, Zhuang Z, Yu Y, Zou Z. A covalent organic framework bearing single Ni sites as a synergistic photocatalyst for selective photoreduction of CO_2 to co. J Am Chem Soc. 2019;141(18):7615.

[80] Haug WK, Wolfson ER, Morman BT, Thomas CM, McGrier PL. A nickel-doped dehydrobenzoannulene-based two-dimensional covalent organic framework for the reductive cleavage of inert aryl C-S bonds. J Am Chem Soc. 2020;142(12):5521.

[81] Yu X, De Waele V, Lofberg A, Ordomsky V, Khodakov AY. Selective photocatalytic conversion of methane into carbon monoxide over zinc-heteropolyacid-titania nanocomposites. Nat Commun. 2019;10:700.

[82] Wang Y, Liu X, Han X, Godin R, Chen J, Zhou W, Jiang C, Thompson JF, Mustafa KB, Shevlin SA, Durrant JR, Guo Z, Tang J. Unique hole-accepting carbon-dots promoting selective carbon dioxide reduction nearly 100% to methanol by pure water. Nat Commun. 2020;11:2531.

[83] Wagner A, Sahm CD, Reisner E. Towards molecular understanding of local chemical environment effects in electro- and photocatalytic CO_2 reduction. Nat Catal. 2020;3(10):775.

[84] Ran J, Jaroniec M, Qiao SZ. Cocatalysts in semiconductor-based photocatalytic CO_2 reduction: achievements, challenges, and opportunities. Adv Mater. 2018;30(7):1704649.

[85] Pati PB, Wang R, Boutin E, Diring S, Jobic S, Barreau N, Odobel F, Robert M. Photocathode functionalized with a molecular cobalt catalyst for selective carbon dioxide reduction in water. Nat Commun. 2020;11:3499.

[86] Jiang Z, Wan W, Li H, Yuan S, Zhao H, Wong PK. A hierarchical z-scheme alpha-Fe_2O_3/g-C_3N_4 hybrid for enhanced photocatalytic CO_2 reduction. Adv Mater. 2018;30(10):1706108.

[87] Gao C, Meng Q, Zhao K, Yin H, Wang D, Guo J, Zhao S, Chang L, He M, Li Q, Zhao H, Huang X, Gao Y, Tang Z. Co_3O_4 hexagonal platelets with controllable facets enabling highly efficient visible-light photocatalytic reduction of CO_2. Adv Mater. 2016;28(30):6485.

[88] Dong C, Lian C, Hu S, Deng Z, Gong J, Li M, Liu H, Xing M, Zhang J. Size-dependent activity and selectivity of carbon dioxide photocatalytic reduction over platinum nanoparticles. Nat Commun. 2018;9:1252.

[89] Chen F, Ma Z, Ye L, Ma T, Zhang T, Zhang Y, Huang H. Macroscopic spontaneous polarization and surface oxygen vacancies collaboratively boosting CO_2 photoreduction on $BiOIO_3$ single crystals. Adv Mater. 2020;32(11):1908350.

[90] Bie C, Zhu B, Xu F, Zhang L, Yu J. In situ grown monolayer N-doped graphene on CdS hollow spheres with seamless contact for photocatalytic CO_2 reduction. Adv Mater. 2019;31(42):1902868.

[91] Bae KL, Kim J, Lim CK, Nam KM, Song H. Colloidal zinc oxide-copper(i) oxide nanocatalysts for selective aqueous photocatalytic carbon dioxide conversion into methane. Nat Commun. 2017;8:1156.

[92] Gong YN, Zhong W, Li Y, Qiu Y, Zheng L, Jiang J, Jiang HL. Regulating photocatalysis by spin-state manipulation of cobalt in covalent organic frameworks. J Am Chem Soc. 2020;142(39):16723.

[93] Yang S, Hu W, Zhang X, He P, Pattengale B, Liu C, Cendejas M, Hermans I, Zhang X, Zhang J, Huang J. 2D covalent organic frameworks as intrinsic photocatalysts for visible light-driven CO_2 reduction. J Am Chem Soc. 2018;140(44):14614.

[94] Liu W, Li X, Wang C, Pan H, Liu W, Wang K, Zeng Q, Wang R, Jiang J. A scalable general synthetic approach toward

ultrathin imine-linked two-dimensional covalent organic framework nanosheets for photocatalytic CO_2 reduction. J Am Chem Soc. 2019;141(43):17431.

[95] Lv H, Sa R, Li P, Yuan D, Wang X, Wang R. Metalloporphyrin-based covalent organic frameworks composed of the electron donor-acceptor dyads for visible-light-driven selective CO_2 reduction. Sci China Chem. 2020;63(9):1289.

[96] Shen J, Kortlever R, Kas R, Birdja YY, Diaz-Morales O, Kwon Y, Ledezma-Yanez I, Schouten KJ, Mul G, Koper MT. Electrocatalytic reduction of carbon dioxide to carbon monoxide and methane at an immobilized cobalt protoporphyrin. Nat Commun. 2015;6:8177.

[97] Kibria MG, Dinh CT, Seifitokaldani A, De Luna P, Burdyny T, Quintero-Bermudez R, Ross MB, Bushuyev OS, Garcia de Arquer FP, Yang P, Sinton D, Sargent EH. A surface reconstruction route to high productivity and selectivity in CO_2 electroreduction toward C_{2+} hydrocarbons. Adv Mater. 2018; 30(49):1804867.

[98] Chen R, Wang Y, Ma Y, Mal A, Gao XY, Gao L, Qiao L, Li XB, Wu LZ, Wang C. Rational design of isostructural 2D porphyrin-based covalent organic frameworks for tunable photocatalytic hydrogen evolution. Nat Commun. 2021;12: 1354.

[99] Zhao Z, Zheng Y, Wang C, Zhang S, Song J, Li Y, Ma S, Cheng P, Zhang Z, Chen Y. Fabrication of robust covalent organic frameworks for enhanced visible-light-driven H_2 evolution. ACS Catal. 2021;11(4):2098.

[100] Zhang FM, Sheng JL, Yang ZD, Sun XJ, Tang HL, Lu M, Dong H, Shen FC, Liu J, Lan YQ. Rational design of MOF/COF hybrid materials for photocatalytic H_2 evolution in the presence of sacrificial electron donors. Angew Chem Int Ed. 2018;57(37):12106.

[101] Zu X, Li X, Liu W, Sun Y, Xu J, Yao T, Yan W, Gao S, Wang C, Wei S, Xie Y. Efficient and robust carbon dioxide electroreduction enabled by atomically dispersed $sn^{\delta+}$ sites. Adv Mater. 2019;31(15):1808135.

[102] Zhu HJ, Lu M, Wang YR, Yao SJ, Zhang M, Kan YH, Liu J, Chen Y, Li SL, Lan YQ. Efficient electron transmission in covalent organic framework nanosheets for highly active electrocatalytic carbon dioxide reduction. Nat Commun. 2020; 11:497.

[103] Zheng T, Jiang K, Wang H. Recent advances in electrochemical CO_2-to-Co conversion on heterogeneous catalysts. Adv Mater. 2018;30(48):1802066.

[104] Xu H, Rebollar D, He H, Chong L, Liu Y, Liu C, Sun CJ, Li T, Muntean JV, Winans RE, Liu DJ, Xu T. Highly selective electrocatalytic CO_2 reduction to ethanol by metallic clusters dynamically formed from atomically dispersed copper. Nat Energy. 2020;5(8):623.

[105] Wang X, de Araujo JF, Ju W, Bagger A, Schmies H, Kuhl S, Rossmeisl J, Strasser P. Mechanistic reaction pathways of enhanced ethylene yields during electroreduction of CO_2-Co co-feeds on Cu and Cu-tandem electrocatalysts. Nat Nanotechnol. 2019;14(11):1063.

[106] Song RB, Zhu W, Fu J, Chen Y, Liu L, Zhang JR, Lin Y, Zhu JJ. Electrode materials engineering in electrocatalytic CO_2 reduction: energy input and conversion efficiency. Adv Mater. 2020;32(27):1903796.

[107] Ma L, Hu W, Mei B, Liu H, Yuan B, Zang J, Chen T, Zou L, Zou Z, Yang B, Yu Y, Ma J, Jiang Z, Wen K, Yang H. Covalent triazine framework confined copper catalysts for selective electrochemical CO_2 reduction: operando diagnosis of active sites. ACS Catal. 2020;10(8):4534.

[108] Wu Q, Xie RK, Mao MJ, Chai GL, Yi JD, Zhao SS, Huang YB, Cao R. Integration of strong electron transporter tetrathiafulvalene into metalloporphyrin-based covalent organic

framework for highly efficient electroreduction of CO_2. ACS Energy Lett. 2020;5(3):1005.

[109] Cheung PL, Lee SK, Kubiak CP. Facile solvent-free synthesis of thin iron porphyrin COFs on carbon cloth electrodes for CO_2 reduction. Chem Mater. 2019;31(6):1908.

[110] Huang N, Lee KH, Yue Y, Xu X, Irle S, Jiang Q, Jiang D. A stable and conductive metallophthalocyanine framework for electrocatalytic carbon dioxide reduction in water. Angew Chem Int Ed. 2020;59(38):16587.

[111] Li J, Chen G, Zhu Y, Liang Z, Pei A, Wu CL, Wang H, Lee HR, Liu K, Chu S, Cui Y. Efficient electrocatalytic CO_2 reduction on a three-phase interface. Nat Catal. 2018;1(8):592.

[112] Liang HQ, Zhao S, Hu XM, Ceccato M, Skrydstrup T, Daasbjerg K. Hydrophobic copper interfaces boost electroreduction of carbon dioxide to ethylene in water. ACS Catal. 2021;11(2): 958.

[113] Zhu YG, Shang CQ, Wang ZY, Zhang JQ, Yang MY, Cheng H, Lu ZG. Co and N co-modified carbon nanotubes as efficient electrocatalyst for oxygen reduction reaction. Rare Met. 2019; 40(1):90.

[114] Zhang Q, Zhang Y, Meng Z, Tong W, Yu X, An Q. Constructing the magnetic bifunctional graphene/titania nanosheet-based composite photocatalysts for enhanced visible-light photodegradation of MB and electrochemical ORR from polluted water. Sci Rep. 2017;7:12296.

[115] Xiao M, Chen Y, Zhu J, Zhang H, Zhao X, Gao L, Wang X, Zhao J, Ge J, Jiang Z, Chen S, Liu C, Xing W. Climbing the apex of the ORR volcano plot via binuclear site construction: electronic and geometric engineering. J Am Chem Soc. 2019; 141(44):17763.

[116] Zhou J, Zhang L, Huang YC, Dong CL, Lin HJ, Chen CT, Tjeng LH, Hu Z. Voltage- and time-dependent valence state transition in cobalt oxide catalysts during the oxygen evolution reaction. Nat Commun. 2020;11:1984.

[117] Wang J, Gao Y, Kong H, Kim J, Choi S, Ciucci F, Hao Y, Yang S, Shao Z, Lim J. Non-precious-metal catalysts for alkaline water electrolysis: operando characterizations, theoretical calculations, and recent advances. Chem Soc Rev. 2020; 49(24):9154.

[118] Zhu Y, Lin Q, Zhong Y, Tahini HA, Shao Z, Wang H. Metal oxide-based materials as an emerging family of hydrogen evolution electrocatalysts. Energ Environ Sci. 2020;13(10): 3361.

[119] Zhang J, Wu J, Guo H, Chen W, Yuan J, Martinez U, Gupta G, Mohite A, Ajayan PM, Lou J. Unveiling active sites for the hydrogen evolution reaction on monolayer MoS_2. Adv Mater. 2017;29(42):1701955.

[120] Yin Y, Zhang Y, Gao T, Yao T, Zhang X, Han J, Wang X, Zhang Z, Xu P, Zhang P, Cao X, Song B, Jin S. Synergistic phase and disorder engineering in $1T-MoSe_2$ nanosheets for enhanced hydrogen-evolution reaction. Adv Mater. 2017; 29(28):1700311.

[121] Wang ZY, Jiang SD, Duan CQ, Wang D, Luo SH, Liu YG. In situ synthesis of Co_3O_4 nanoparticles confined in 3D nitrogen-doped porous carbon as an efficient bifunctional oxygen electrocatalyst. Rare Met. 2020;39(12):1383.

[122] Li T, Hu T, Dai L, Li CM. Metal-free photo- and electro-catalysts for hydrogen evolution reaction. J Mater Chem A. 2020; 8(45):23674.

[123] Huang H, Yan M, Yang C, He H, Jiang Q, Yang L, Lu Z, Sun Z, Xu X, Bando Y, Yamauchi Y. Graphene nanoarchitectonics: recent advances in graphene-based electrocatalysts for hydrogen evolution reaction. Adv Mater. 2019;31(48):1903415.

[124] Hua W, Sun HH, Xu F, Wang JG. A review and perspective on molybdenum-based electrocatalysts for hydrogen evolution reaction. Rare Met. 2020;39(4):335.

[125] Suen NT, Hung SF, Quan Q, Zhang N, Xu YJ, Chen HM. Electrocatalysis for the oxygen evolution reaction: recent development and future perspectives. Chem Soc Rev. 2017; 46(2):337.

[126] Wang J, Wang J, Qi S, Zhao M. Stable multifunctional single-atom catalysts resulting from the synergistic effect of anchored transition-metal atoms and host covalent–organic frameworks. J Phys Chem C. 2020;124(32):17675.

[127] Zhao X, Pachfule P, Li S, Langenhahn T, Ye M, Schlesiger C, Praetz S, Schmidt J, Thomas A. Macro/microporous covalent organic frameworks for efficient electrocatalysis. J Am Chem Soc. 2019;141(16):6623.

[128] Guo J, Lin CY, Xia Z, Xiang Z. A pyrolysis-free covalent organic polymer for oxygen reduction. Angew Chem Int Ed. 2018;57(38):12567.

[129] Park E, Jack J, Hu Y, Wan S, Huang S, Jin Y, Maness PC, Yazdi S, Ren Z, Zhang W. Covalent organic framework-supported platinum nanoparticles as efficient electrocatalysts for water reduction. Nanoscale. 2020;12(4):2596.

[130] Ding Y, Cai P, Wen Z. Electrochemical neutralization energy: from concept to devices. Chem Soc Rev. 2021;50(3):1495.

[131] Vaghasiya JV, Mayorga-Martinez CC, Pumera M. Flexible energy generation and storage devices: focus on key role of heterocyclic solid-state organic ionic conductors. Chem Soc Rev. 2020;49(21):7819.

[132] Yi F, Ren H, Shan J, Sun X, Wei D, Liu Z. Wearable energy sources based on 2D materials. Chem Soc Rev. 2018;47(9):3152.

[133] Tian XL, Zhao X, Su YQ, Wang LJ, Wang HM, Dang D, Chi B, Liu HF, Hensen EJM, Lou XW, Xia BY. Engineering bunched Pt-Ni alloy nanocages for efficient oxygen reduction in practical fuel cells. Science. 2019;366(6467):850.

[134] Qiao MF, Wang Y, Li L, Hu GZ, Zou GA, Mamat X, Dong YM, Hu X. Self-templated nitrogen-doped mesoporous carbon decorated with double transition-metal active sites for enhanced oxygen electrode catalysis. Rare Met. 2019;39(7):824.

[135] Singh SK, Takeyasu K, Nakamura J. Active sites and mechanism of oxygen reduction reaction electrocatalysis on nitrogen-doped carbon materials. Adv Mater. 2019;31(13):1804297.

[136] Wang S, Zhang Z, Zhang H, Rajan AG, Xu N, Yang Y, Zeng Y, Liu P, Zhang X, Mao Q, He Y, Zhao J, Li BG, Strano MS, Wang WJ. Reversible polycondensation-termination growth of covalent-organic-framework spheres, fibers, and films. Matter. 2019;1(6):1592.

[137] Tan J, Namuangruk S, Kong W, Kungwan N, Guo J, Wang C. Manipulation of amorphous-to-crystalline transformation: towards the construction of covalent organic framework hybrid microspheres with NIR photothermal conversion ability. Angew Chem Int Ed. 2016;55(45):13979.

[138] Fan H, Gu J, Meng H, Knebel A, Caro J. High-flux membranes based on the covalent organic framework COF-LZU1 for selective dye separation by nanofiltration. Angew Chem Int Ed. 2018;57(15):4083.

[139] Kandambeth S, Biswal BP, Chaudhari HD, Rout KC, Kunjattu HS, Mitra S, Karak S, Das A, Mukherjee R, Kharul UK, Banerjee R. Selective molecular sieving in self-standing porous covalent-organic-framework membranes. Adv Mater. 2017; 29(2):1603945.

[140] Khan NA, Zhang R, Wu H, Shen J, Yuan J, Fan C, Cao L, Olson MA, Jiang Z. Solid-vapor interface engineered covalent organic framework membranes for molecular separation. J Am Chem Soc. 2020;142(31):13450.

[141] Wang J, Huang Z, Liu W, Chang C, Tang H, Li Z, Chen W, Jia C, Yao T, Wei S, Wu Y, Li Y. Design of N-coordinated dual-metal sites: a stable and active Pt-free catalyst for acidic oxygen reduction reaction. J Am Chem Soc. 2017;139(48):17281.

[142] Yun R, Zhan F, Wang X, Zhang B, Sheng T, Xin Z, Mao J, Liu S, Zheng B. Design of binary Cu-Fe sites coordinated with nitrogen dispersed in the porous carbon for synergistic CO_2 electroreduction. Small. 2021;17(4):e2006951.

[143] Kim H, Shin D, Yang W, Won DH, Oh HS, Chung MW, Jeong D, Kim SH, Chae KH, Ryu JY, Lee J, Cho SJ, Seo J, Kim H, Choi CH. Identification of single-atom Ni site active toward electrochemical CO_2 conversion to CO. J Am Chem Soc. 2021; 143(2):925.

[144] Wei H, Ning J, Cao X, Li X, Hao L. Benzotrithiophene-based covalent organic frameworks: construction and structure transformation under ionothermal condition. J Am Chem Soc. 2018;140(37):11618.

Xiao-Feng Lin is an associate professor in School of Chemical Engineering and Light Industry at Guangdong University of Technology. He received the Ph. D. degree under the supervision of Prof. Xudong Chen in Polymer Chemistry and Physics from Sun Yat-Sen University in 2018. He was also a visiting scholar under the supervision of Prof. Liming Dai in Department of Macromolecular Science and Engineering at Case Western Reserve University in 2018. His research focuses on controlled synthesis and characterization of polymer composites for opto-electric and opto-thermal conversions.

Ding-Shan Yu received his Ph.D. degree in optical engineering in 2008 from Sun Yat-Sen University (China). After postdoctoral training at the University of Dayton (USA), Case Western Reserve University (USA), and Nanyang Technological University (Singapore), he joined Sun Yat-sen University as a professor in 2015. His research interests include design and synthesis of polymeric functional composites and carbon materials as well as their applications in optoelectronic devices and energy storage and conversion system.